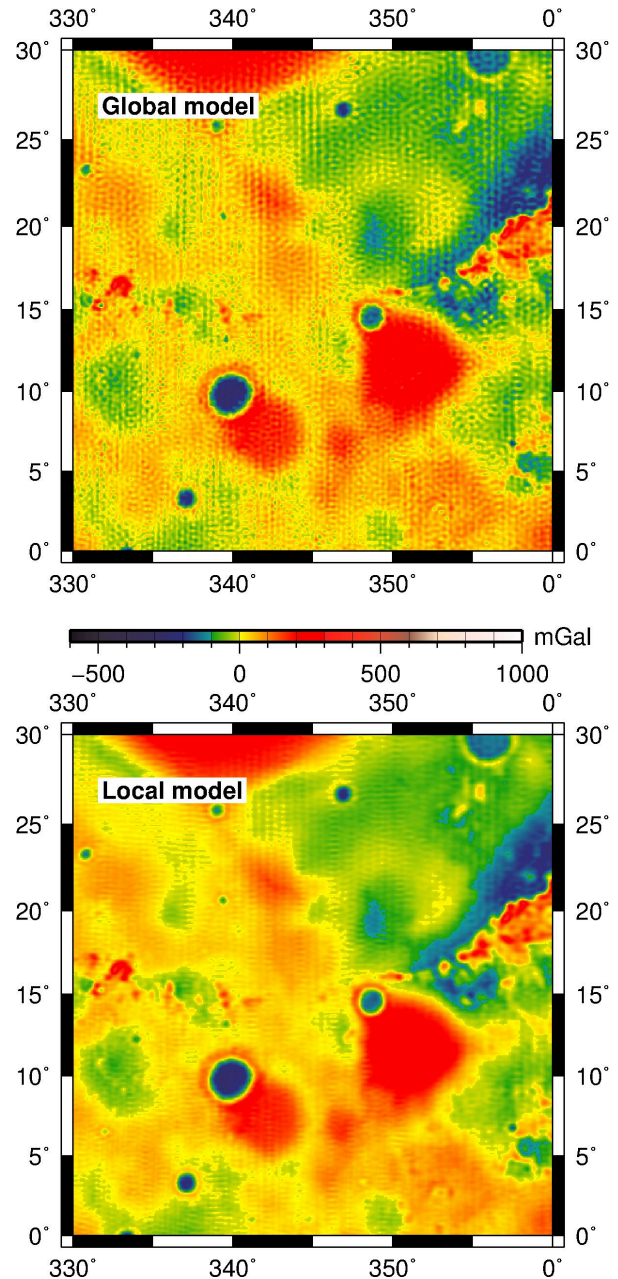


**A HIGH-RESOLUTION GLOBAL MAP OF LUNAR GRAVITY FROM PATCHED LOCAL SOLUTIONS USING GRAIL DATA.** Sander Goossens<sup>1,2</sup>, Terence Sabaka<sup>2</sup>, Álvaro Fernández Mora<sup>1,2,3</sup>, Eduard Heijkoop<sup>1,2,3</sup>. <sup>1</sup>Center for Research and Exploration in Space Science and Technology, University of Maryland Baltimore County, Baltimore MD, USA (email: [sander.j.goossens@nasa.gov](mailto:sander.j.goossens@nasa.gov)); <sup>2</sup>NASA GSFC, Code 698, Greenbelt MD, USA; <sup>3</sup>Delft University of Technology, Faculty of Aerospace Engineering, Delft, The Netherlands.

**Introduction:** The primary science objectives of the Gravity Recovery and Interior Laboratory (GRAIL) mission are to determine the structure of the lunar interior from crust to core and to advance the understanding of the thermal evolution of the Moon [1,2]. These objectives are to be achieved by producing a high-quality, high-resolution map of the gravitational field of the Moon. The concept of the GRAIL mission and its measurements is based on the successful GRACE mission which mapped the gravity field of the Earth [3]: the distance between two co-orbiting spacecraft was measured precisely using a Ka-band ranging system (KBRR) [4], augmented by tracking from Earth using the Deep Space Network (DSN) [5].

The GRAIL mission consisted of two separate phases: a primary mission phase, which lasted from March 1, 2012 until May 29, 2012, where the spacecraft were at an average altitude of 50 km above lunar surface, and an extended mission phase, which lasted from August 30, 2012, until December 14, 2012, during which the average spacecraft altitude was 23 km. In the latter part of the extended mission this altitude was lowered further to 20 km (November 18) and finally 11 km (December 6). Using these data, several models expressed in spherical harmonics have been determined, with current maximum resolutions of degree and order 1200 [6] or 1500 [7]. However, the effective resolution of these models varies spatially because of varying spacecraft altitude and ground track spacing. Global spherical harmonics are not optimal when the spatial data coverage is heterogeneous, because they require smoothness constraints that are commonly applied to the entire model, resulting in the underestimation of especially peak amplitudes. In such instances, local methods of gravity recovery are advantageous. Here, we present the results of a fully localized analysis of GRAIL tracking data, resulting in a global map of lunar gravity that delineates features clearer than an equivalent global model, and that has improved correlations with the Lunar Reconnaissance Orbiter's Lunar Orbiter Laser Altimeter (LOLA) topography [8].

**Methods:** We have implemented a localized method that uses gridded gravity anomalies (to describe gravity signal in addition to the background global model), which are estimated from KBRR data only, selected above the area of interest. We have demonstrated this method for a solution covering the south pole of the Moon [9]. We determine the satellite orbits using both KBRR and DSN data for a span of on



**Figure 1** Anomalies from a global model in spherical harmonics (top) and our local solution (bottom). The local solution shows small scale features much more clearly.

average two and a half days. From these orbits, we select the times that the satellite pair's ground track covers the area of interest, which results in spans (called

arcs) much shorter than the initial arcs (on average their duration is  $\sim 22$  minutes). We redetermine the orbits for these short arcs using only KBRR data, where we transform the coordinates of the satellites' position and velocity into those describing the baseline of the vector between them [10]. We only determine 3 out of the 12 possible coordinates because it has been shown that KBRR data are most sensitive to these coordinates [10]: the pitch of the GRAIL A-B position baseline, the magnitude of the GRAIL A-B velocity baseline, and the pitch of the GRAIL A-B velocity baseline. When these orbits are redetermined, we generate partial derivatives of the KBRR measurements with respect to the gravity anomalies. We then form a system of normal equations to estimate the anomalies. We apply a neighbor smoothing constraint to this system [11,12], where we smooth the full gravity anomaly, which consists of the contribution of the global background model and the new adjustments. Applying this constraint to the full anomalies instead of to the adjustments only has several advantages [9]: it results in smoother maps of gravity, and improved correlations with topography (see also Fig.).

In addition, we have investigated how to patch together local solutions for separate areas into one map covering the complete Moon. Local methods often suffer from boundary effects, because data close to the boundary of the area are in principle also affected by gravity anomalies outside the area of interest that are not estimated. We thus extend our local solutions such that they are overlapping with neighboring areas. We then combine neighboring solutions by discarding 5 degrees around the edges of both solutions. The areas have been selected such that with this deletion the resulting anomalies match up perfectly with the neighboring solutions, thus constituting a complete global map without duplicate anomalies. We have showed that this method of combination results in the best correlations with topography.

**Results:** We selected 14 areas covering the complete Moon, including two caps that cover the poles. A local solution for each area was determined completely independent of all the other areas. The resolution of each map is  $0.15^\circ$  by  $0.15^\circ$ , which is equivalent to a degree and order 1200 model in spherical harmonics. For each solution, we applied different weight factors to the data normal equation system and the constraint normal equation system separately. We generated 9 different solutions for each area (a combination of 3 different weights for low-altitude December data, and 3 different weights for the constraint system, resulting in 9 different combinations of weights), and selected the solution with the best localized correlations [13] with topography for each local area. We then patched these solutions into a global map (see Fig.). In addition, we transformed the

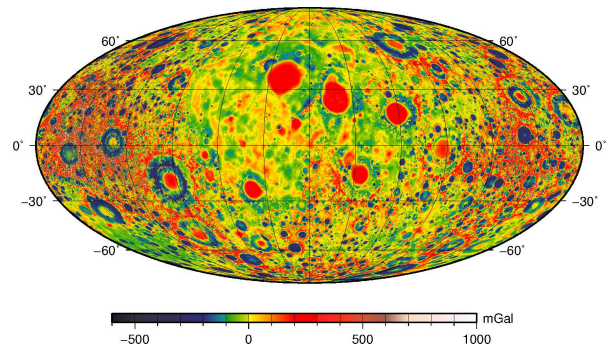


**Figure 2** Our global map of lunar gravity, at a resolution of  $0.15^\circ$  by  $0.15^\circ$ , consisting of patched local solutions.

anomaly map into spherical harmonics. Using the spherical harmonic coefficients, we can compute correlations with topography, and Bouguer corrections with filters in the spherical harmonic domain. The global map from local solutions shows improved correlations with topography. Details in the gravity field are less affected by striping when compared to the global models. This makes the resulting model suitable for density studies of craters and the lunar crust at small scales. The computation of local solutions is computationally less intensive than determining a global model in spherical harmonics of equivalent size. In addition, we can be more versatile with the constraints, selecting the optimum smoothing per area.

We will archive the separate local solutions as free-air anomaly maps, and we will archive the resulting spherical harmonic expansion.

**References:** [1] Zuber M. T. *et al.* (2012), *Science*, doi: 10.1126/ science.1231507. [2] Zuber M. T. *et al.* (2013), *Space Sci. Rev.*, doi:10.1007/s11214-012-9952-7. [3] Tapley B. D. *et al.* (2004), *Science*, doi:10.1126/science.1099192. [4] Klipstein *et al.* (2013), *Space Sci. Rev.*, doi:10.1007/s11214-013-9973-x. [5] Asmar S.W. *et al.* (2013), *Space Sci. Rev.*, doi: 10.1007/s11214-013-9962-0. [6] Goossens, S. *et al.* (2016), *LPSC XLVII*, abstract 1484. [7] Park, R.S. *et al.* (2015), American Geophysical Union, Fall Meeting, San Francisco, abstract #G41B-01. [8] Smith, D.E. *et al.* (2017), *Icarus*, doi:10.1016/j.icarus.2016.06.006. [9] Goossens S. *et al.* (2014), *Geophys. Res. Lett.*, doi: 10.1002/2014 GL060178. [10] Rowlands D.D. (2002) *J. Geod.*, doi: 10.1007/s00190-002-0255-8. [11] Rowlands D.D. *et al.* (2010), *J. Geophys. Res.*, doi: doi:10.1029/2009JB006546. [12] Sabaka T. J. *et al.* (2010), *J. Geophys. Res.*, doi:10.1029/2010JB007533. [13] Wieczorek M. A. and Simons F. J. (2005), *Geophys. J. Int.*, doi:10.1111/j. 1365-246X.2005.02687.x.